International Journal of Heat and Mass Transfer 52 (2009) 3628–3633

Contents lists available at ScienceDirect

International Journal of Heat and Mass Transfer

journal homepage: www.elsevier.com/locate/ijhmt

Constructal ducts with wrinkled entrances

T. Bello-Ochende [a], J.P. Meyer [a,*], A. Bejan [b]

[a] Department of Mechanical and Aeronautical Engineering, University of Pretoria, Pretoria 0002, South Africa
[b] Department of Mechanical Engineering and Materials Science, Duke University, Box 90300, Durham, NC 27708-300, USA

ARTICLE INFO

Article history:
Received 3 March 2008
Accepted 17 March 2009
Available online 22 April 2009

Keywords:
Wrinkled entrance
Constructal theory
Laminar flow
Optimal duct size

ABSTRACT

This paper reports an increase in the heat transfer rate density by using wrinkled entrance regions in ducts with laminar flow. The heat transfer rate density is increased by taking advantage of the presence of relative isothermal fluid in the entrance regions. In order to stimulate a more complete thermal interaction between walls and fluid, the square entrances are wrinkled on the perimeter, at the one-third and the two-third positions. The new structure has two degrees of freedom. The fluid flow through the ducts is forced by the imposed pressure difference along the duct. Numerical simulations document the effects of the dimensionless pressure drop on the optimized configurations, and show a 15% enhancement in heat transfer rate density.

1. Introduction

The use of progressively smaller length scales for heat transfer in ducts and channels is attracting considerable interest [1–17]. The need to install more and more heat transfer in a fixed volume has led to various new methods and designs. One method that is drawing interest is constructal design [1]. The method focuses on the generation of flow architecture as a mechanism by which systems achieve greater transport density under constraints. Constructal design offers strategies for the pursuit of configuration, such that architectural features which were found to be beneficial in the past can be refined and incorporated into complex systems [2–4].

The constructal design of packages of channels began with the research by Bejan and Sciubba [5], which determined the optimal spacing for arrays of parallel plates using the intersection of asymptotes method. The application was the cooling of electronics packages. Optimal spacings for heat and fluid flow structures have been developed for several classes of flow configurations: stacks of parallel plates, staggered plates, cylinders in cross-flow, and pin fin arrays with impinging flow. Optimal spacings have been determined for natural convection and for forced convection with specified overall pressure difference. Most recently, Yilmaz et al. [17] and Muzychka [15] analytically determined the optimal duct dimensions and maximum heat transfer rate per unit volume for parallel plate channels, rectangular channels, elliptic ducts, circular ducts, polygonal ducts, and triangular ducts.

In this paper, we propose a new concept to improve the constructal design for the cooling of a duct. We start with a square packing of channels, Fig. 1. The size of the square ducts is to be selected numerically subject to fixed pressure drop across the packing. The entrance regions of the duct do not participate fully in the heat transfer enterprise, because of the presence of relatively isothermal (cold) fluid that has not interacted thermally with the walls. Next, the duct entrance is wrinkled to stimulate a more complete thermal interaction between walls and fluid. The new structure has two degrees of freedom: the downstream length of the wrinkled entrance, and the spacing of the square ducts. These geometric features are optimized for maximum volumetric heat transfer density.

2. Model

Consider the three-dimensional configuration of a channel with a wrinkled perimeter around a square cross-section. Fig. 2 shows the entrance of one square channel after each side was wrinkled at the one-third and two-thirds positions. The walls of the channels (including the wrinkled portions) are maintained at the temperature T_{max}. The channel is cooled by a single-phase fluid at T_{min}, which is forced into the channel by a specified pressure difference (ΔP). The coolant is modelled as a Newtonian fluid with constant properties. The dimensionless equations for the steady-state flow of mass, momentum and energy are

$$\frac{\partial \tilde{u}}{\partial \tilde{x}}+\frac{\partial \tilde{v}}{\partial \tilde{y}}+\frac{\partial \tilde{w}}{\partial \tilde{z}}=0 \tag{1}$$

$$\frac{\mathrm{Be}}{Pr}\left(\tilde{u}\frac{\partial \tilde{u}}{\partial \tilde{x}}+\tilde{v}\frac{\partial \tilde{u}}{\partial \tilde{y}}+\tilde{w}\frac{\partial \tilde{u}}{\partial \tilde{z}}\right)=-\frac{\partial \tilde{P}}{\partial \tilde{x}}+\nabla^2\tilde{u} \tag{2}$$

$$\frac{\mathrm{Be}}{Pr}\left(\tilde{u}\frac{\partial \tilde{v}}{\partial \tilde{x}}+\tilde{v}\frac{\partial \tilde{v}}{\partial \tilde{y}}+\tilde{w}\frac{\partial \tilde{v}}{\partial \tilde{z}}\right)=-\frac{\partial \tilde{P}}{\partial \tilde{y}}+\nabla^2\tilde{v} \tag{3}$$

$$\frac{\mathrm{Be}}{Pr}\left(\tilde{u}\frac{\partial \tilde{w}}{\partial \tilde{x}}+\tilde{v}\frac{\partial \tilde{w}}{\partial \tilde{y}}+\tilde{w}\frac{\partial \tilde{w}}{\partial \tilde{z}}\right)=-\frac{d\tilde{P}}{d\tilde{z}}+\nabla^2\tilde{w} \tag{4}$$

$$\mathrm{Be}\left(\tilde{u}\frac{\partial \tilde{T}}{\partial \tilde{x}}+\tilde{v}\frac{\partial \tilde{T}}{\partial \tilde{y}}+\tilde{w}\frac{\partial \tilde{T}}{\partial \tilde{z}}\right)=\nabla^2\tilde{T} \tag{5}$$

* Corresponding author. Tel.: +27 12 420 2590; fax: +27 12 362 5124.
E-mail address: jmeyer@up.ac.za (J.P. Meyer).

0017-9310/$ - see front matter © 2009 Elsevier Ltd. All rights reserved.
doi:10.1016/j.ijheatmasstransfer.2009.03.014

Nomenclature

Be	dimensionless pressure drop, Eq. (6)
D	side of square cross-section, m
k	thermal conductivity, W/mK
L_0	length in the flow direction, m
L_1	flow length of the wrinkled section, m
P	pressure, Pa
Pr	Prandtl number
q	heat transfer rate, W
q'''	heat transfer rate density
$\tilde{q}$	dimensionless heat transfer density
Re	Reynolds number
T	temperature, K
T_{wall}	wall temperature, K
T_{min}	free-stream temperature, K
U	mean velocity, m/s
u, v, w	velocity component, m/s
x, y, z	cartesian coordinates, m

Greek letters

α	thermal diffusivity, m^2/s
μ	viscosity, kg/s m
γ	convergence criterion

Subscripts

L_1	length
max	maximum
min	minimum
opt	optimum
wall	wall
∞	free-stream

Superscript

$\sim$	dimensionless

where $\nabla^2 = \partial^2/\partial\tilde{x}^2 + \partial^2/\partial\tilde{y}^2 + \partial^2/\partial\tilde{z}^2$, and the dimensionless pressure difference is defined as [11,12]:

$$\mathrm{Be} = \frac{\Delta P L_0^2}{\mu\alpha} \tag{6}$$

The non-dimensionalization of the governing equations is based on defining the variables

$$\tilde{x}, \tilde{y}, \tilde{z} = \frac{(x, y, z)}{L_0}, \quad \tilde{P} = \frac{P}{\Delta P} \tag{7}$$

$$(\tilde{u}, \tilde{v}, \tilde{w}, \tilde{U}) = \frac{(u, v, w, U)}{\Delta P L_0/\mu}, \quad \tilde{T} = \frac{T - T_{min}}{T_{wall} - T_{min}} \tag{8}$$

The boundary conditions are

$$\tilde{P} = 1, \quad \tilde{v} = \tilde{w} = 0, \quad \tilde{T} = 0 \text{ at } \tilde{x} = 0 \tag{9}$$

$$\tilde{u} = \tilde{v} = \tilde{w} = 0, \quad \tilde{T} = 1 \text{ on the walls} \tag{10}$$

$$\tilde{P} = 0 \text{ at } \tilde{x} = 1 \tag{11}$$

Zero normal stress at the outlet ($\tilde{x} = 1$) of the duct and the remaining portions of the boundary was modeled as adiabatic, and

$$\tilde{D} = \frac{D}{L_0} \tag{12}$$

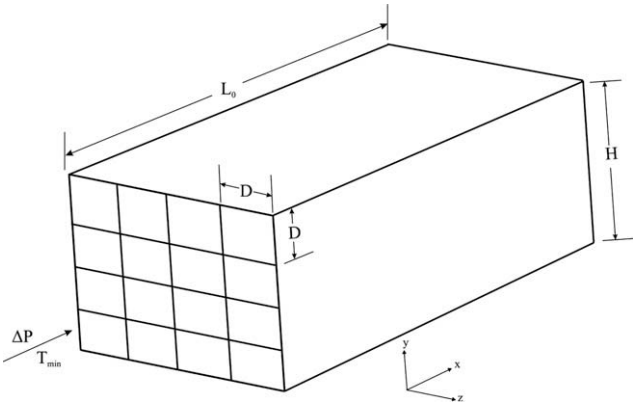

Fig. 1. Packing of channels with square cross-sections.

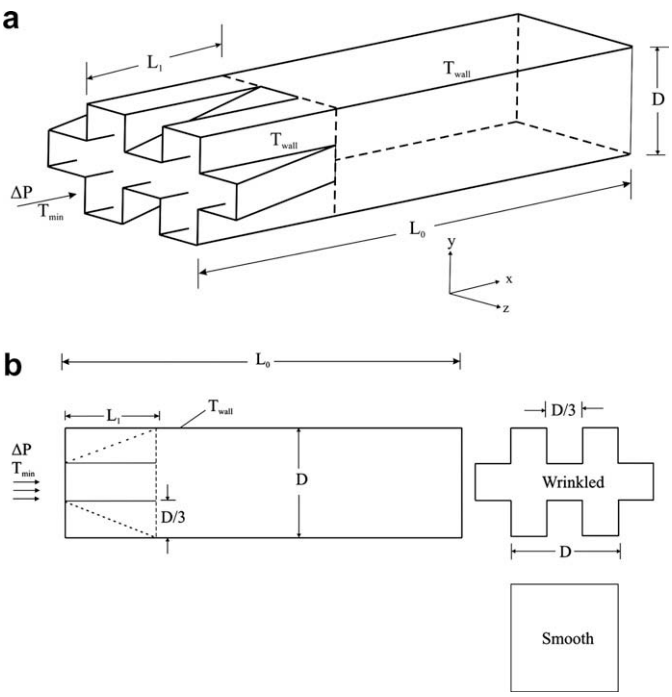

Fig. 2. Entrance of a square channel wrinkled at the 1/3 and 2/3 positions.

We are interested in the geometric arrangement of the wrinkled packing for which the overall heat transfer rate per unit of flow volume is maximum:

$$q''' = \frac{\text{total heat transfer rate from walls to stream}}{\text{volume of one duct}} = \frac{q}{L_0 D^2} \tag{13}$$

In dimensionless form, the above definition can be rewritten as

$$\tilde{q} = \frac{qL_0}{k(T_w - T_\infty)D^2} \tag{14}$$

We solved Eqs. (2)–(5) by using a commercial finite volume code [18]. The domain was discretized using tetrahedral elements, and the governing equations were integrated at every control volume. Second-order schemes were used for the diffusive terms. The

pressure velocity coupling was performed with the SIMPLE procedure. Convergence was obtained when the normalized residuals for the mass and momentum equations were smaller than 10^{-4}, and the residual of the energy equation became smaller than 10^{-8}.

To obtain accurate numerical results, several mesh refinement tests were conducted. The monitored quantity was the overall heat transfer rate density, which was computed with Eq. (14). Convergence was established based on the criterion

$$\gamma = |\tilde{q}_j - \tilde{q}_j - 1|/|\tilde{q}_j| \leq 0.02 \tag{15}$$

where j is the mesh iteration index, such that j increases when the mesh is more refined. When the criterion is satisfied, the $j-1$ mesh is selected as the converged mesh. A mesh size of 0.005 per unit length in the y- and z-directions, and a mesh size of 0.01 per unit length in the axial direction were found to satisfy the criterion chosen in Eq. (15).

3. Results

We started the optimization procedure by considering the case in which the mouth of the square channel is smooth, without wrinkles. In this case, the only degree of freedom is the duct size, $\tilde{D}$. Fig. 3 shows the selection of the channel size and the heat transfer rate density, and indicates that an optimal size exists for a channel with a square packing.

The optimal square channel was found for a fixed dimensionless pressure drop number Be in the range of 10^5–10^8, and a Prandtl number of 0.71. These initial results were compared with the available literature to validate the numerical code. The procedure was repeated several times to cover the range $10^5 \leqslant \mathrm{Be} \leqslant 10^8$. Fig. 3 shows that the variation of channel sizes reveals a maximum heat transfer rate density. The optimum size for $\mathrm{Be} = 10^5$ is located between $\tilde{D} = 0.24$ and 0.25 on the abscissa.

To enhance the heat transfer rate density, we wrinkled the mouths of the square channel in order to bring the walls closer to the unused core fluid. The total volume of the wrinkled duct is the same as that of the smooth duct. The new structure has two degrees of freedom. The dimensionless length of the fold and the side of the square cross-section are defined as

$$\tilde{L}_1 = \frac{L_1}{L_0} \tag{16}$$

The optimization was executed in the following sequence: we first assumed values of $\tilde{D}$ and $\tilde{L}_1$, using as initial guess the optimal values of $\tilde{D}$ obtained when there were no wrinkles. The optimization was performed in two nested loops, because of the two degrees of freedom, $\tilde{D}$ and $\tilde{L}_1$. In the inner loop, the values of Be, Pr, and $\tilde{D}$ (wrinkled) were specified, and $\tilde{L}_1$ was varied until a maximum heat transfer rate density was reached. The outer loop required that the inner loop was repeated for several values of $\tilde{D}$, such that all the possible combinations of $\tilde{D}$ and $\tilde{L}_1$ were analyzed, as shown in Fig. 4. The resulting heat transfer rate density was maximized with respect to both $\tilde{D}$ and $\tilde{L}_1$. The above procedure was repeated for Be in the range of $10^5 \leqslant \mathrm{Be} \leqslant 10^8$.

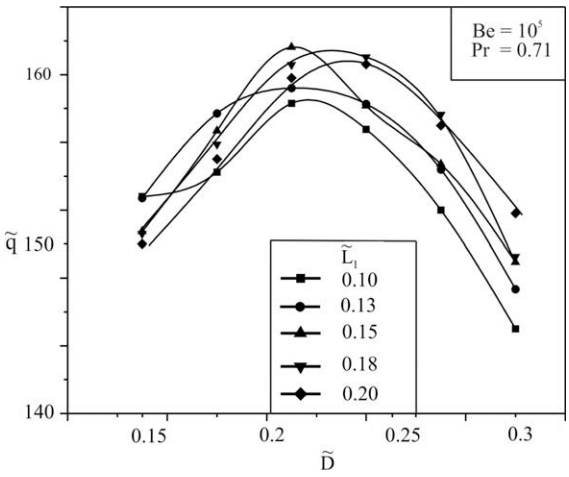

Fig. 4. The effect of $\tilde{L}_1$ and $\tilde{D}$ (wrinkled) on the heat transfer density.

Fig. 5 shows the behaviour of the optimized length scales as the Be number changes. The optimized length scale ($\tilde{L}_{1,\mathrm{opt}}$) increases with the dimensionless pressure drop number. The slenderness of the channel also increases in this direction. The optimal duct size decreases as the dimensionless pressure drop increases. The optimal duct sizes for the wrinkled and smooth ducts are almost the same. The results presented in Fig. 5 are correlated by

$$\begin{aligned} \tilde{D}_{\mathrm{smooth,opt}} &\cong 3.27\mathrm{Be}^{-0.24} \\ \tilde{D}_{\mathrm{wrinkled,opt}} &\cong 2.73\mathrm{Be}^{-0.22} \\ \tilde{L}_{1,opt} &= 0.067\mathrm{Be}^{0.068} \end{aligned} \tag{17}$$

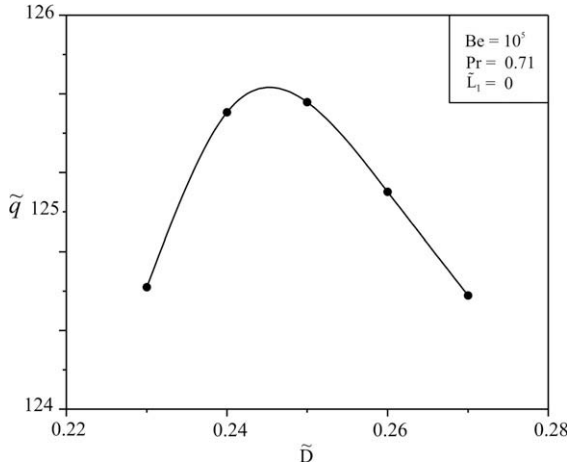

Fig. 3. Effect of the channel size $\tilde{D}$ (smooth) on the heat transfer density.

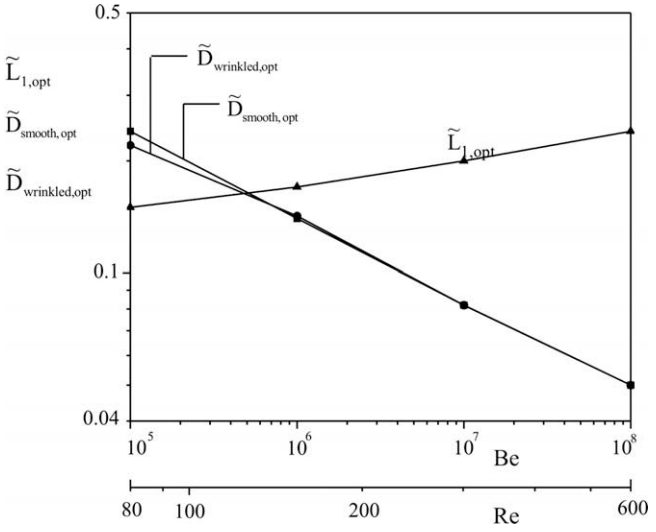

Fig. 5. Effect of dimensionless pressure difference on the optimized length scales.

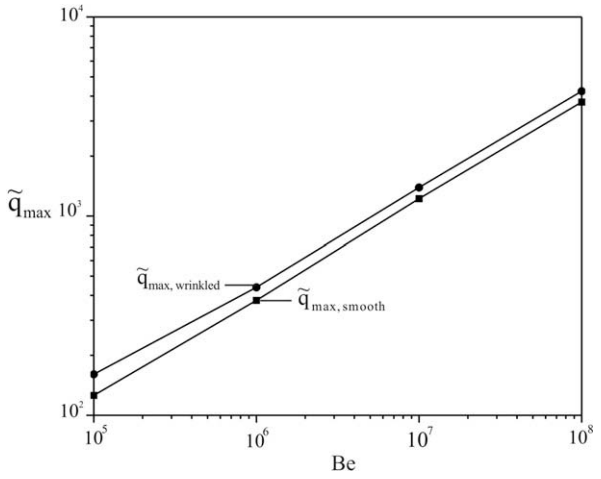

Fig. 6. Effect of dimensionless pressure difference on the heat transfer rate density.

This behaviour is in agreement with previous results for optimal spacings for square channels [15]. The assumption of laminar flow is validated by calculating the Reynolds number based on the mean velocity and optimal duct size based on the smooth ducts.

$$Re = \frac{\rho U D_{\text{smooth, opt}}}{\mu} = \tilde{U}\tilde{D}_{\text{smooth,opt}}\frac{\text{Be}}{Pr} \tag{18}$$

Eq. (18), shows the relationship between the dimensionless pressure drop number Be, the mean velocity, the optimal duct size and the Prandtl number. By determining $\tilde{U}$ and $\tilde{D}_{\text{smooth,opt}}$ numerically, we found that the Reynolds numbers of the flows lie in the laminar regime (Fig. 5). Expressed in terms of *Re*, the results are correlated as

$$\begin{aligned}\tilde{D}_{\text{smooth,opt}} &\cong 8.16Re^{-0.80}\\ \tilde{D}_{\text{wrinkled,opt}} &\cong 6.54Re^{-0.77}\\ \tilde{L}_{1,\text{opt}} &= 0.051Re^{0.24}\end{aligned} \tag{19}$$

Fig. 6 shows the variation of the maximal heat transfer rate density for the wrinkled and the smooth ducts. Both increase with the dimensionless pressure difference. When Be is in the range of 10^5–10^6, the heat transfer density increases by 17% in going from the optimized smooth duct to the optimized wrinkled duct. The increase is 13% for Be in the range of 10^7–10^8. The results of Fig. 6 are correlated by

$$\begin{aligned}q_{\text{max,smooth}} &\cong 0.38\text{Be}^{1/2}\\ q_{\text{max,wrinkled}} &\cong 0.45\text{Be}^{1/2}\end{aligned} \tag{20}$$

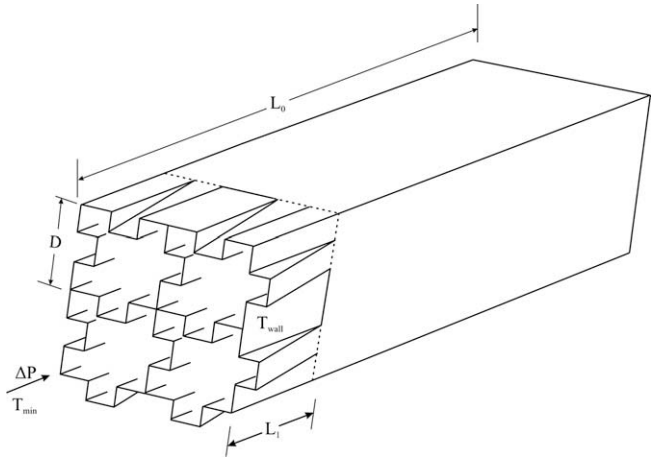

Fig. 7. Packing of channels with wrinkled square cross-sections.

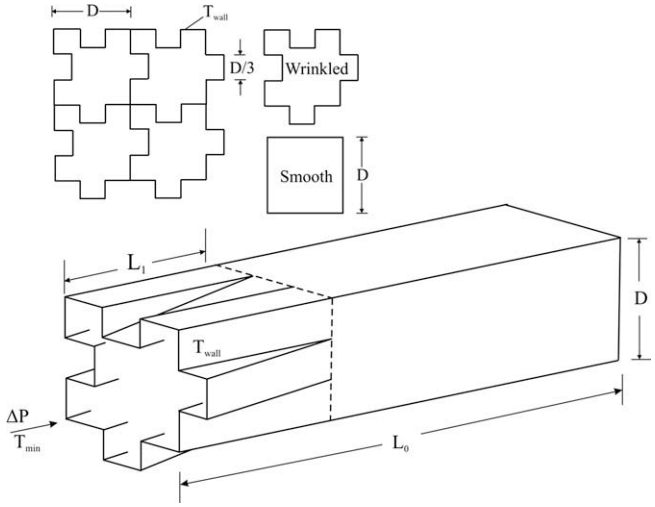

Fig. 8. Packing of wrinkled square entrances showing an elemental computational unit of a square channel with wrinkled entrances.

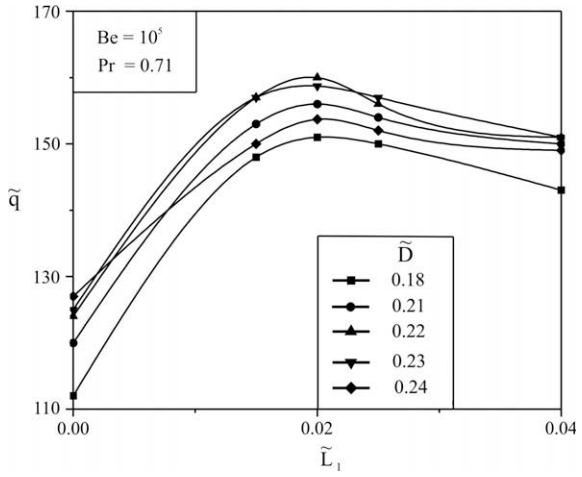

Fig. 9. The effect of $\tilde{L}_1$ and $\tilde{D}$ (wrinkled) on the heat transfer density in the assembly of Fig. 8.

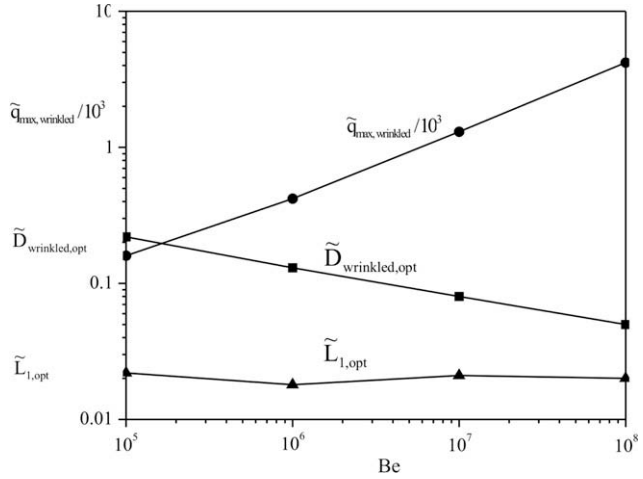

Fig. 10. The effect of dimensionless pressure difference on the optimized length scales and on the heat transfer rate density on the assembly of Fig. 8.

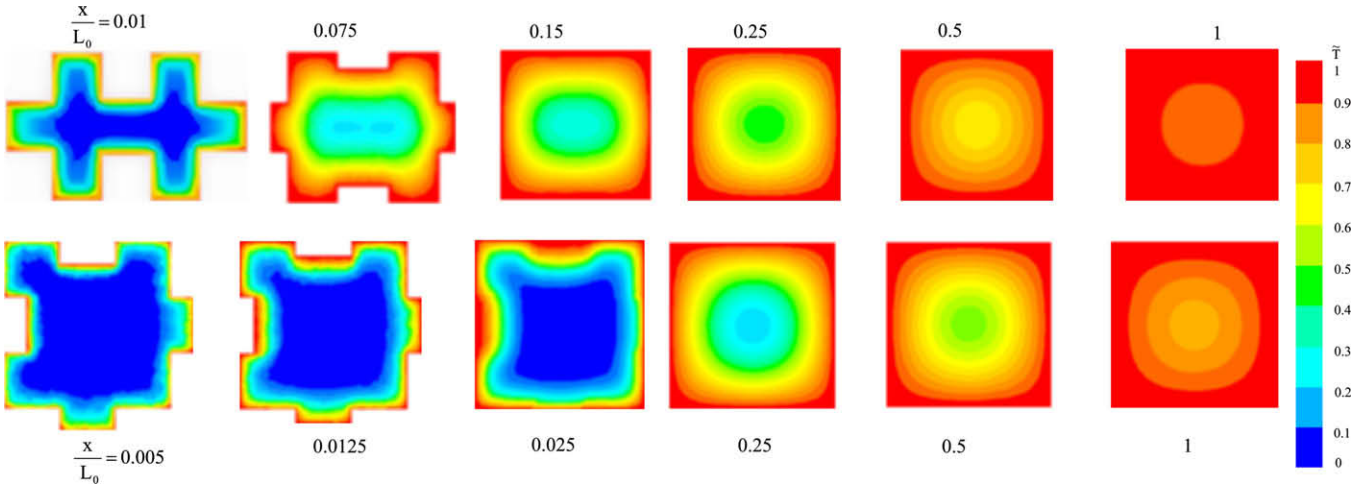

Fig. 11. The temperature distribution at the entrance, midsection and outlet of the optimized wrinkled ducts (top) and modified wrinkled ducts (bottom), for $Be = 10^5$.

The trend is similar to the results of Muzychka [15] and the earlier work on the optimal spacing for convection [1]. The 13–17% increase in heat transfer rate density is consistent with the increase achieved in Ref. [3] by inserting shorter (optimal) plates in the entrance region of stacks of parallel plate channels.

4. Packing of wrinkled ducts

In the second phase of this study, we considered a modified type of wrinkling which allowed us to pack the wrinkled entrances into a larger assembly, as shown in Figs. 7 and 8. The number of degrees of freedom of the geometry is the same as before, namely two. The only change is the depth of the wrinkled section, which is kept fixed at $\tilde{D}/6$, in order for the total volume of the new design to be the same as that of smooth ducts, and to prevent the wrinkled walls from touching. These modifications prevent numerical instabilities and allow the flow to fill the entrance. Any changes in the position ($\tilde{D}/6$) result in increases or decreases in the total volume when compared with the total volume of a smooth tube of comparable size.

The numerical procedure for flow simulation and geometry optimization was the same as the procedure tested in Section 2. As shown in the example of Fig. 9, the Be number was fixed, and many configurations of $(\tilde{D}, \tilde{L}_1)$ were simulated in search of the configuration with the highest heat transfer density $\tilde{q}$. This procedure was then repeated over the range of $10^5 \leqslant Be \leqslant 10^8$.

The results for the new wrinkled duct are reported in Fig. 10. They show the new optimized square cross-section, the optimized length of the fold and the maximized performance, and how they vary with the dimensionless pressure difference. The optimal length of the fold ($\tilde{L}_{1,opt}$) shows little variation with Be. The optimal duct size decreases as Be increases, and this behaviour is consistent with what we saw in Fig. 5. The heat transfer rate density for the winkled ducts of Fig. 8 is almost the same as that of Fig. 2: the difference is within 1%.

Fig. 11 shows the temperature distributions of optimized wrinkled ducts at several axial locations for $Be = 10^5$ and $Pr = 0.71$. The figure shows the evolution of the temperature distributions as the axial distance increases. The temperature ranges between two colours, red ($\tilde{T} = 1$) and blue ($\tilde{T} = 0$). As the axial distance increases, the colour at the central plane of the wrinkled ducts changes from blue at the wrinkled entrance to red at the exit (square).

5. Conclusions

In this paper, we described a new design for increasing the heat transfer rate density by using wrinkled entrance regions in ducts with laminar forced convection. The method consists of wrinkling the perimeter of the square entrances, and extending these deformations gradually downstream to a length ($\tilde{L}_1$), which is optimized. This new geometry allows a more complete heat transfer interaction between the walls and the fluid. The results show that the heat transfer rate density increases with the imposed pressure difference (Be). In the wrinkled geometry, the optimal length of the fold increases with Be, in accord with results reported in the literature for multiscale packages of parallel plates. We developed a second wrinkled geometry such that many such channels can be packed fully into a larger volume. In this modified wrinkled geometry, the effect of Be on the optimal length on the fold is weak. The results show an increase of 15% in heat transfer rate density in going from smooth ducts to wrinkled ducts.

Acknowledgements

Tunde Bello-Ochende acknowledges the support of the University of Pretoria, Research Development Programme (RDP). Adrian Bejan acknowledges the support received from the Air Force Office of Scientific Research through a grant for "Constructal technology for thermal management of aircraft".

References

[1] A. Bejan, S. Lorente, Design with Constructal Theory, Wiley, Hoboken, NJ, 2008.
[2] T. Bello-Ochende, A. Bejan, Maximal heat transfer density: plates with multiple lengths in forced convection, Int. J. Therm. Sci. 43 (2004) 1181–1186.
[3] A. Bejan, Y. Fautrelle, Constructal multi-scale structure for maximal heat transfer density, Acta Mech. 163 (2003) 39–49.
[4] A.K. da Silva, A. Bejan, Constructal multi-scale structure for maximal heat transfer density in natural convection, Int. J. Heat Fluid Flow 26 (2005) 34–44.
[5] A. Bejan, E. Sciubba, The optimal spacing for parallel plates cooled by forced convection, Int. J. Heat Mass Transfer 35 (1992) 3259–3264.
[6] S.J. Kim, S.W. Lee (Eds.), Air Cooling Technology for Electronic Equipment, CRC Press, Boca Raton, FL, 1996 (Chapter 1).
[7] J.-M. Koo, S. Im, L. Jiang, K.E. Goodson, Integrated microchannel cooling for three-dimensional electronic architectures, J. Heat Transfer 127 (2005) 49–58.
[8] R.S. Matos, T.A. Laursen, J.V.C. Vargas, A. Bejan, Three-dimensional optimization of staggard finned circular and elliptic tubes in forced convection, Int. J. Therm. Sci. 43 (2004) 447–487.
[9] S.K.W. Tou, C.P. Tso, X. Zhang, 3D numerical analysis of natural convective cooling of a 3×3 heater array in rectangular enclosures, Int. J. Heat Mass Transfer 44 (1999) 3231–3244.

[10] S. Bhattacharjee, W.L. Grosshandler, The formation of a wall jet near a high temperature wall under microgravity environment, ASME HTD 96 (1988) 711–716.
[11] S. Petrescu, Comments on the optimal spacing of parallel plates cooled by forced convection, Int. J. Heat Mass Transfer 37 (1994) 1283.
[12] T. Bello-Ochende, L. Liebenberg, A.G. Malan, A. Bejan, J.P. Meyer, Constructal conjugate heat transfer in three-dimensional cooling channels, J. Enhanc. Heat Transfer 14 (4) (2007) 279–293.
[13] W. Nakayama, H. Matsushima, P. Goel, Forced convective heat transfer from arrays of finned packages, in: W. Aung (Ed.), Cooling Technology for Electronic Equipment, Hemisphere, New York, 1988, pp. 195–210.
[14] T. Bello-Ochende, A. Bejan, Constructal multi-scale cylinders in cross-flow, Int. J. Heat Mass Transfer 48 (2005) 1373–1383.
[15] Y.S. Muzychka, Constructal design of forced convection cooled microchannel heat sinks and heat exchangers, Int. J. Heat Mass Transfer 48 (2005) 3119–3127.
[16] T. Bello-Ochende, L. Liebenberg, J.P. Meyer, Constructal cooling channels for microchannel heat sinks, Int. J. Heat Mass Transfer 50 (2007) 4141–4150.
[17] A. Yilmaz, O. Buyukalaca, T. Yilmaz, Optimum shape and dimensions of ducts for convective heat transfer in laminar flow at constant wall temperature, Int. J. Heat Mass Transfer 43 (2000) 767–775.
[18] www.fluent.com.